

Design, Synthesis, and Molecular Mechanism Studies of *N*-Phenylisoxazoline-thiadiazolo[3,4-*a*]pyridazine Hybrids as Protoporphyrinogen IX Oxidase Inhibitors

Rui-Bo Zhang, Shu-Yi Yu, Lu Liang, Ismail Ismail, Da-Wei Wang,* Yong-Hong Li, Han Xu, Xin Wen, and Zhen Xi*



Cite This: <https://dx.doi.org/10.1021/acs.jafc.0c05955>



Read Online

ACCESS |



Metrics & More



Article Recommendations



Supporting Information

ABSTRACT: Protoporphyrinogen oxidase (PPO, EC 1.3.3.4) is an important target for green agrochemical discovery. Herein, a novel *N*-phenylisoxazoline-thiadiazolo[3,4-*a*]pyridazine herbicidal active scaffold was designed by the scaffold hybridization strategy. Systematic structural optimization enabled the discovery of a series of derivatives with excellent weed control at 9.375–150 g ai/ha by the post-emergent application. Some derivatives exhibited improved *Nicotiana tabacum* PPO (NtPPO)-inhibitory activity than fluthiacet-methyl. Of these, **2b**, with $K_i = 21.8$ nM, displayed higher weed control than fluthiacet-methyl at the rate of 12–75 g ai/ha, and selective to maize at 75 g ai/ha. *In planta*, **2b** was converted into a bioactive metabolite **5** ($K_i = 4.6$ nM), which exhibited 4.6-fold more potency than **2b** in inhibiting the activity of NtPPO. Molecular dynamics simulation explained that **5** formed stronger π – π interaction with Phe392 than that of **2b**. This work not only provides a promising lead compound for weed control in maize fields but is also helpful to understand the molecular mechanism and basis of the designed hybrids.

KEYWORDS: molecular mechanism, molecular simulation, phenylisoxazoline, protoporphyrinogen IX oxidase, proherbicide

INTRODUCTION

Weeds aggressively compete with crops for space, nutrients, light, and water, decimating yields and causing annual losses of more than \$100 billion around the world.¹ To date, it remains a challenge to effectively control undesirable vegetations that grow within crops. Although herbicides can control unwanted plants in fields, however, improper and long-term irrational use of some herbicides, such as triazines and glyphosate, has caused serious environmental problems and led to the emergence of herbicide-resistant weeds.^{2–4} Therefore, new herbicides with an environmentally benign character and improved herbicidal activity are in demand. Protoporphyrinogen oxidase (PPO, EC 1.3.3.4) is one of the most vital targets for green herbicide research; it catalyzes protoporphyrinogen IX to protoporphyrin IX in the presence of O₂. Protoporphyrin IX is not only a precursor for the biosynthesis of chlorophyll but also a photosensitizer that can generate singlet oxygen species upon exposure to light.^{5–8} Inhibition of PPO will lead to the accumulation of protoporphyrin IX in the plant cell, which eventually results in the peroxidative destruction of cell membranes and plant death. To date, there are more than 30 commercialized PPO-inhibiting herbicides, which can further be divided into diphenylethers, uracils, thiadiazoles, oxadiazoles, triazolinones, phenylpyrazole, and *N*-phenylphthalimides.^{9,10}

Fluthiacet-methyl is a thiadiazole-type PPO herbicide (Figure 1), which has been used for the control of post-emergent annual broadleaf weeds (including the resistant weed *Palmer amaranth*) in soybean and maize fields.¹¹ It can effectively control many sensitive weeds at an extremely low

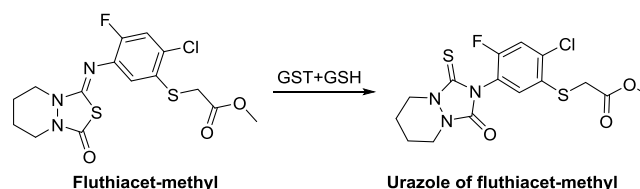


Figure 1. Isomerization of fluthiacet-methyl to urazole of fluthiacet-methyl in the presence of glutathione (GSH) by GST.

use rate of 5 to 10 g ai/ha. Unlike other PPO herbicides that inhibit PPO *in vivo*, fluthiacet-methyl has been classified as a proherbicide¹² because it was found that *in planta*, fluthiacet-methyl can be transformed into urazole of fluthiacet-methyl by glutathione S-transferase (GST) (Figure 1).¹³ The same isomerization can also be observed by incubation of fluthiacet-methyl and glutathione (GSH) with GST. Both fluthiacet-methyl and urazole showed strong PPO-inhibitory activity; however, the detailed molecular basis of PPO inhibition of these two types of compounds is especially lacking.

Interestingly, different types of PPO inhibitors have conflicting structure–activity relationships. The possible

Received: September 16, 2020

Revised: October 13, 2020

Accepted: October 27, 2020

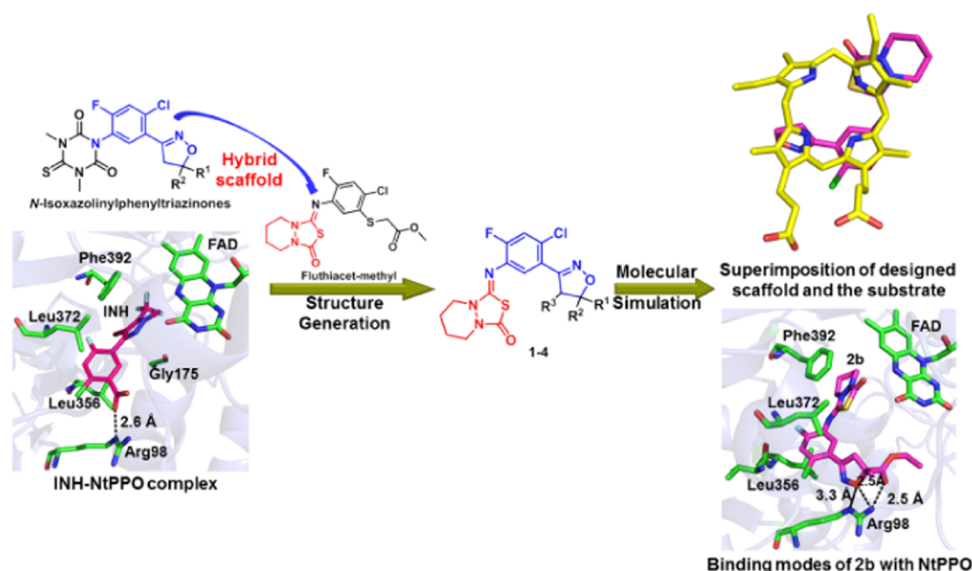
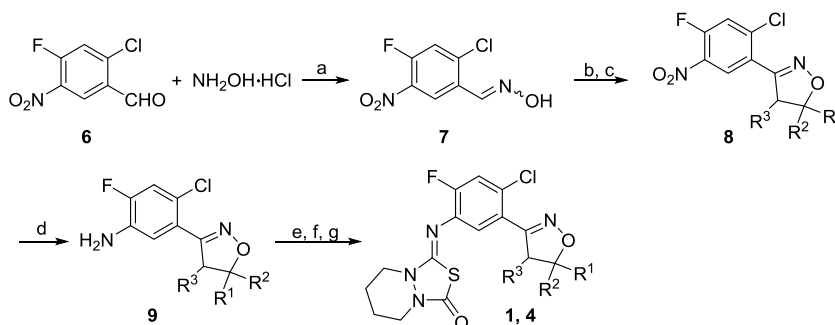


Figure 2. Design strategy of *N*-phenylisoxazoline-thiadiazolo[3,4-*a*]pyridazines. The main residues in the active site of NtPPO are highlighted as green sticks, and the backbone of NtPPO is shown as light blue cartoons. INH is shown as red sticks, **2b** is shown as magenta sticks, and the substrate protoporphyrinogen IX is presented as yellow sticks.

Scheme 1. Synthesis of Compounds **1** and **4**^a



^aReagents and conditions: (a) $\text{C}_2\text{H}_5\text{OH}$, H_2O , 0 °C room-temperature (rt); (b) *N*-chlorosuccinimide (NCS), *N,N*-dimethylformamide (DMF), 35 °C; (c) $\text{CH}_2=\text{CR}^1\text{R}^2$ or $\text{R}^2\text{HC}=\text{CHR}^3$, Et_3N , CH_2Cl_2 , 0 °C; (d) Fe , NH_4Cl , $\text{C}_2\text{H}_5\text{OH}$ (90%), reflux; (e) CSCl_2 , Et_3N , toluene, 0 °C-reflux; (f) hexahydropyridazine dihydrochloride, NaOH , toluene, H_2O , 0 °C; and (g) $\text{CO}(\text{OCCl}_3)_2$, Et_3N , acetone, 0 °C.

reason may be that these compounds are competitive inhibitors, and their structures can overlay with two or three pyrrole rings of protoporphyrinogen IX.^{14–17} In 2004, Koch et al. reported the crystal structure of *Nicotiana tabacum* PPO (NtPPO) in complex with a phenylpyrazole-type inhibitor 4-Bromo-3-(*S*'-carboxy-4'-chloro-2'-fluoro-phenyl)-1-methyl-5-trifluoromethyl-pyrazol (INH).¹⁸ They found that INH can mimic half of the structure of protoporphyrinogen IX upon binding to the active site. There were mainly three interactions of INH with NtPPO: the first was the π – π interaction between the pyrazole ring of INH with Phe392, the second was the hydrophobic interactions of the benzene ring with Leu372 and Leu356, and the third was the hydrogen-bonding interactions of Arg98 with the carbonyl group of INH (Figure 2). These interactions not only play a crucial role in improving the PPO-inhibitory activity of INH but also provide new insights for designing novel PPO inhibitors.^{9,19–21}

Many studies have shown that for the *N*-phenylheterocycle PPO-inhibiting herbicides, compounds with 2-fluoro-4-chloro-5-substituted-phenyl substitution patterns would show higher bioactivity than their corresponding analogues with chlorine, bromine, and hydrogen atoms at the 2-position of the benzene

ring.²² We recently reported a series of highly efficient *N*-isoxazolinylphenyltriazinone PPO inhibitors. Among them, compounds with a fluorine atom at the 2-position and a chlorine atom at the 4-position of the benzene ring were found to show superior herbicidal and PPO inhibition activities.²³ Therefore, designing novel inhibitors based on the 2-fluoro-4-chloro-5-isoxazolinylphenyl motif may provide an effective strategy for discovering new herbicides. In this study, we applied a scaffold hopping strategy by hybridizing the 2-fluoro-4-chloro-5-isoxazolinylphenyl motif with the thiadiazolo[3,4-*a*]pyridazine function group and designed a series of compounds **1–4** based on the *N*-phenylisoxazoline-thiadiazolo[3,4-*a*]pyridazine scaffold (Figure 2). Systematic herbicidal activity and PPO-inhibitory activity evaluation of **1–4** led to compound **2b**, which exhibited an excellent and wide spectrum of weed control. Additionally, to explore interaction mechanisms, we have performed systematic molecular dynamic (MD) simulations studies of compounds **2b** and **5** with NtPPO.

Table 1. Post-Emergent Herbicidal Activity and NtPPO-Inhibitory Activity of Compounds 1a–c

compd	R ¹	R ²	R ³	dosage g ai/ha	% inhibition				K _i /nM	cLogP
					ABUJU ^a	AMARE	ECHCG	DIGSA		
1a	H	–CO ₂ CH ₂ CH ₃	H	150	100	100	58	74	38 ± 7.4	4.4
				37.5	100	100	58	69		
				18.75	100	100	33	57		
				9.375	100	100	0	54		
1b	CH ₃	–CH ₂ OCOCH ₃	H	150	100	100	41	21	4.8 ± 1.4	4.3
				37.5	100	100	46	45		
				18.75	100	100	40	38		
				9.375	100	98	31	27		
1c	CH ₃	–CH ₂ CH ₃	H	150	100	100	90	42	38 ± 9.4	5.4
				37.5	100	100	66	56		
				18.75	100	100	63	51		
				9.375	100	99	50	30		
fluthiacet-methyl			H	37.5	100	100	52	46	15 ± 0.2	3.8
				18.75	100	99	33	37		
				9.375	100	89	20	0		

^aAbbreviations: ABUJU: *A. juncea*; AMARE: *A. retroflexus*; DIGSA: *D. sanguinalis*; and ECHCG: *E. crus-galli*.

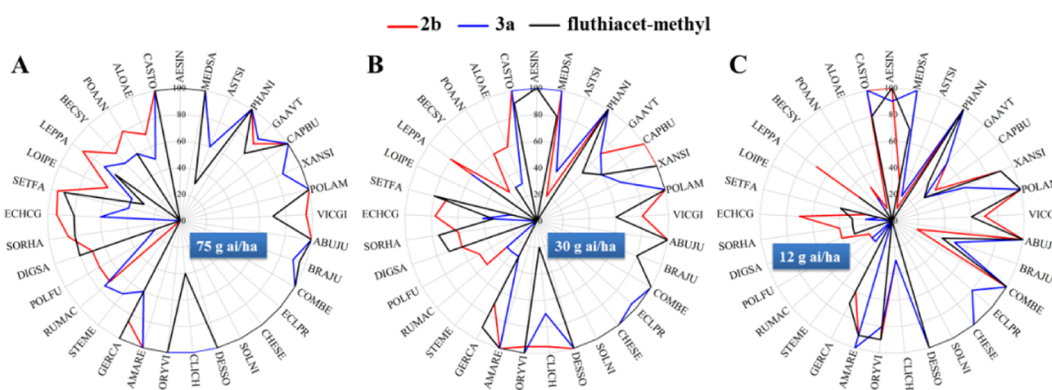


Figure 3. Post-emergent herbicidal spectrum of representative compounds **2b** and **3a**. (A) Herbicidal spectrum at 75 g ai/ha; (B) herbicidal spectrum at 30 g ai/ha; and (C) herbicidal spectrum at 12 g ai/ha. Abbreviations: AESIN, *A. indica*; ASTSI, *A. sinicus*; PHANI, *P. nil*; GAAVT, *Galium aparine* var. *tenerum*; CAPBU, *B. juncea*; XANSI, *X. sibiricum*; POLAM, *P. americana*; VICGI, *Vicia gigantea*; ABUJU, *A. juncea*; BRAJU, *B. juncea*; COMBE, *C. benghalensis*; ECLPR, *E. prostrata*; CHESE, *C. serotinum*; SOLNI, *S. nigrum*; DESSO, *D. sophia*; CLICH, *C. chinense*; ORYVI, *O. violaceus*; AMARE, *A. retroflexus*; GERCA, *G. carolinianum*; STEME, *S. media*; RUMAC, *R. acetosa*; POLFU, *P. fugax*; DIGSA, *D. sanguinalis*; SORHA, *S. halepense*; ECHCG, *E. crus-galli*; SETFA, *S. faberii*; LOIPE, *L. perenne*; LEPPA, *Leptochloa panicea*; BECSY, *B. syzigachne*; POAN, *P. annuas*; ALOAE, *A. aequalis*; and CASTO, *C. tora*.

MATERIALS AND METHODS

Synthesis of Compounds 1–5. The chemical synthesis of **1–5** is described in Schemes 1–3, and the synthetic methods of these compounds were similar to our previous method.²³ The detailed synthetic procedures, ¹H and ¹³C NMR, and high-resolution mass spectra (HRMS) of **1–4** are presented in the Supporting Information.

Synthesis of Compound 5. A solution of hexahydropyridazine dihydrochloride (3.0 mmol) and triethylamine (9.0 mmol) in CH₂Cl₂ (20 mL) was stirred at room temperature for 30 min. Then, the mixture was cooled to 0 °C and ethyl chloroacetate (1.5 mmol) in dichloromethane (20 mL) was added dropwise over 10 min. The reaction was stirred at 0 °C for 1 h; after the reaction was completed, CH₂Cl₂ (40 mL) and H₂O (10 mL) were added to the solution. The organic layer was separated and washed with H₂O (20 mL) and saturated NaCl solution (30 mL), dried over anhydrous Na₂SO₄, and concentrated under reduced pressure. The residue was dissolved in 30 mL of toluene.

Then, a solution of **16** (3.0 mmol) in toluene (30 mL) was added dropwise to the above solution. The resulting solution was stirred at room temperature for 3 h, Et₃N (9.0 mmol) was added into the solution, and stirred overnight. After the reaction was completed, ethyl acetate (40 mL) and H₂O (10 mL) were added to the solution. The organic layer was separated and washed with H₂O (20 mL) and

saturated NaCl solution (30 mL), dried over anhydrous Na₂SO₄, concentrated in vacuo, and purified by flash chromatography to give **5**. Yellow oil; yield 50.8%; ¹H NMR (400 MHz, CDCl₃) δ 7.79 (dd, *J* = 7.6, 2.8 Hz, 1H), 7.37 (d, *J* = 9.2 Hz, 1H), 4.26 (q, *J* = 7.2 Hz, 2H), 4.00 (dt, *J* = 17.2, 7.2 Hz, 3H), 3.72 (d, *J* = 5.2 Hz, 2H), 3.38 (dd, *J* = 17.6, 7.2 Hz, 1H), 2.02–1.94 (m, 4H), 1.71 (s, 3H), 1.32 (t, *J* = 7.2 Hz, 3H); ¹³C NMR (101 MHz, CDCl₃) δ 171.55, 171.54, 169.01, 159.49, 156.89, 154.39, 151.17, 135.22, 135.13, 132.47, 132.40, 125.73, 125.68, 119.58, 119.55, 119.42, 119.35, 119.32, 87.07, 87.05, 62.21, 62.14, 62.08, 46.56, 46.52, 45.96, 44.41, 23.31, 23.26, 21.91, 21.57, 14.12, 14.08; HRMS (QFT-ESI) calcd for C₁₉H₂₁ClFN₄O₄S [M + H]⁺ 455.0956, found: 455.0952.

Herbicide Activity. Based on the herbicidal potency of the synthesized compounds, we performed two rounds of herbicidal activity assays. Initially, we evaluated the herbicidal activity of compounds **1–5** against the representative grass weeds *Digitaria sanguinalis* (DIGSA) and *Echinochloa crus-galli* (ECHCG), and broadleaf weeds *Amaranthus tricolor* (AMATR) and *Abutilon juncea* (ABUJU) at 9.375–150 g ai/ha by the post-emergent application. Subsequently, 33 kinds of weeds, *Aeschynomene indica* (AESIN), *Astragalus sinicus* (ASTSI), *Pharbitis nil* (PHANI), *Galium aparine* var. *tenerum* (GAAVT), *Brassica juncea* (CAPBU), *Xanthium sibiricum* (XANSI), *Polygonum americana* (POLAM), *Vicia gigantea*

(VICGI), *A. juncea* (ABUJU), *B. juncea* (BRAJU), *C. benghalensis* (COMBE), *Eclipta prostrata* (ECLPR), *Chenopodium serotinum* (CHESE), *Solanum nigrum* (SOLNI), *Descurainia sophia* (DESSO), *Clinopodium chinense* (CLICH), *Orychophragmus violaceus* (ORYVI), *Amaranthus retroflexus* (AMARE), *Geranium carolinianum* (GERCA), *Stellaria media* (STEME), *Rumex acetosa* (RUMAC), *Polypogon fugax* (POLFU), *D. sanguinalis* (DIGSA), *Sorghum halepense* (SORHA), *E. crus-galli* (ECHCG), *Setaria faberii* (SETFA), *Lolium perenne* (LOIPE), *Leptochloa panicea* (LEPPA), *Beckmannia syzigachne* (BECSY), *Poa annuas* (POAAN), *Alopecurus aequalis* (ALOE), and *Cassia tora* (CASTO), were used in the post-emergence herbicidal spectrum assay at 12–75 g ai/ha. The assay methods were the same as those in our previous reports.^{20,24–27} Briefly, plastic pots (diameter = 7.5 cm) were filled with clay soil to 3/4 of their depth; then, the seeds of tested weeds were planted in the pots and grown in a greenhouse. The test compounds were dissolved in dimethylformamide (DMF) and diluted with a 0.1% Tween-80 solution. When the weeds reached the three-leaf stage, the solutions of the test compounds were sprayed on leaves of the weeds, with three replications for each compound and concentration. Fluthiacet-methyl was used as a positive control and the test solution (Tween-80 + DMF) was used as a blank control. After 21 days, the herbicidal activity of the tested compounds was evaluated, and the results are shown in Tables 1–4 and Figure 3.

Crop Selectivity. Sixteen compounds 2a–d, 2f–i, 2j, 2l–m, 2r–u, and 3a–c with excellent broadleaf weed control were selected for further crop safety assay. Maize, soybean, sorghum, wheat, peanut, and rice were selected as representative crops, and the assay methods were similar to those previously reported.^{9,21,23,28} Briefly, the seeds of tested crops were planted in plastic pots and grown in a greenhouse. The experiment was conducted when the crops reached the four-leaf stage. The tested compounds were applied at 75 g ai/ha, with three replicates for each compound. After 25 days, the crop damage of each compound was evaluated, and the results are presented as percent injury (Table 5).

NtPPO-Inhibitory Activity. *N. tabacum* mitochondrial PPO2 (NtPPO) is a model enzyme widely used in the PPO inhibition assay.^{9,19,21,23,29} The expression and purification of NtPPO have been described in previous work,¹⁸ and the NtPPO inhibition assays were performed as described previously,³⁰ with slight modifications.^{21,23} Briefly, a test solution containing 0.00001–200 μ M inhibitors, 0–35 μ g of recombinant NtPPO protein, 1 mM ethylenediaminetetraacetic acid (EDTA), 5 μ M FAD, 100 mM potassium phosphate buffer (PBS, pH 7.4), 0.03% Tween-80 (v/v), 5 mM dithiothreitol (DTT), and 200 mM imidazole was added to a 96-well black plate (Thermo). The reaction was initiated by adding 0.5–3 μ M protoporphyrinogen IX. The fluorescence intensity was recorded under excitation of 410 nm and emission of 630 nm. Each compound was analyzed three times independently.

Stability Test of 2b and 5 in NtPPO Activity Assay Solution. A reaction solution (400 μ L) containing 200 μ M 2b or 5, 200 μ L of water, 66 μ L of the assay buffer, 20 μ g of NtPPO, and 1.8 μ M protoporphyrinogen IX was incubated at 25 °C for 2.5, 5, and 5 min, respectively.³¹ Then, 135 μ L of methanol was added to the solution and the solution was centrifuged at 12 000g for 5 min. The supernatant was further analyzed by high-performance liquid chromatography (HPLC) (Agilent 1200 Infinity Series) using a C18 column (4.6 \times 150 mm, 5.0 μ m). Other conditions for HPLC were as follows: detection wavelength: 254 nm; mobile phases V_{CH_3CN}/V_{H_2O} = 60:40, and the water phase contained 0.1% CH_3COOH ; and flow rate: 1 mL/min. At least three repetitions were made for each compound and time.

Reactions of 2b with Reducing Agents. A solution (1 mL) containing 100 μ M 2b, 10 mM L-cysteine (Cys), glutathione (GSH), dithiothreitol (DTT), or derine (Ser), Tris-HCl (20 mM, pH 8.0), and 225 μ L of methanol was incubated at 25 °C.¹³ The time course of degradation of 2b and generation of 5 was detected by HPLC every 1 h. The HPLC conditions used in this assay were the same as those described in the above section.

Metabolism of 2b in ECHCG and ABUJU. ECHCG and ABUJU were selected as the representative weeds in the metabolism assay. The five-leaf-stage ECHCG and ABUJU were treated with a solution of 2b (100 μ M, containing 1% Tween-80 and DMF) and then moved to the greenhouse.²³ After about 2 h, the leaves of ABUJU started to drop. About 10 g of the ECHCG and ABUJU leaves were cut. The leaves were then washed with 50 mL of H_2O containing 1% Tween-80 and DMF two times and 50 mL of H_2O once. After removing the water by filter paper, the leaves were triturated together with liquid nitrogen, and the residue was transferred to a flask. H_2O (50 mL) and 100 mL of ethyl acetate were added to the flask and the mixture was stirred vigorously at room temperature for 30 min. The organic layer was separated and concentrated in vacuo. The residue was analyzed using UPLC-HRMS (Waters AcquityUPLC H-class, WatersXevo G2-XS Q-TOF).

Molecular Simulations. cLogP Calculation. The three-dimensional (3D) structures of compounds 1–5 and fluthiacet-methyl were constructed and optimized using Sybyl 6.9 (Tripos, Inc.); then, the optimized structures were used for the cLogP calculation.^{32,33}

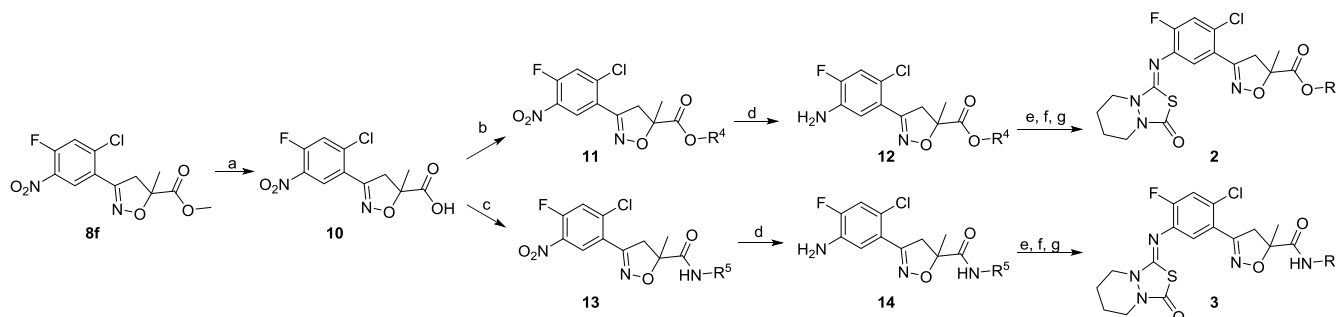
Structural Alignments. The structures of protoporphyrinogen IX and the *N*-phenylisoxazoline-thiadiazolo[3,4-*a*]pyridazine scaffold were constructed and optimized using Sybyl 6.9, the alignment of two molecules was performed using Open3DALIGN,³⁴ and the results were visualized using PYMOL 1.3.³⁵

Molecular Docking. The structures of NtPPO (pdb id: 1sez) were used for the molecular docking and molecular dynamics (MD) simulation study. Before docking, the water molecules, emulsifier, and ligand were stripped using PYMOL. The Kollman charges and hydrogen atoms were added to the protein using AutoDockTools.³⁶ AutoDock 4.2 was applied for docks R-2b, S-2b, R-5, and S-5 into the active site of NtPPO. For each compound, a total of 500 docking runs were performed. The Lamarckian genetic algorithm was used for conformational search; other parameters were set as the default values. The best binding mode of each ligand was selected according to the docking score and referenced to the conformation of INH.

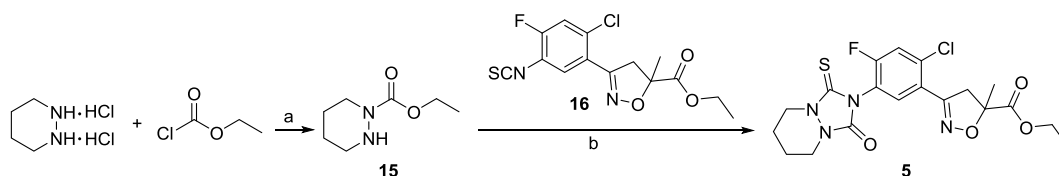
MD Simulations. MD simulations of the ligand–protein complexes were performed using the AMBER 14 software package with ff14SB force fields.³⁷ The Antechamber program was used to generate AMBER force fields (GAFF) for the ligands.³⁸ Each of the ligand–protein systems was solvated with explicit TIP3P water molecules in an 8.0 Å truncated octahedral box; the system was neutralized by adding Cl^- . Before MD simulations, the hydrogen atoms and the side chains of the molecular systems were relaxed.⁵ The steepest descent and conjugate gradient methods were performed to perform energy minimization of the complexes. The ligand–protein systems were gently heated from 0 to 300 K over 50 ps, and a 50 ps equilibrating calculation was performed at 1 atm and 300 K. Finally, a 30 ns MD simulation of each complex was performed. The snapshots in the last 10 ns of MD simulation were used for the binding free-energy calculation, and the results are shown in Table S1. The energy decomposition analysis of each system was performed using the mm_pbsa module.

RESULTS AND DISCUSSION

Exploring the Structures of *N*-Phenylisoxazoline-thiadiazolo[3,4-*a*]pyridazine Hybrids. As we have mentioned in the introduction, PPO inhibitors often share conflicting SAR rules. Our previous work has shown that installing a fluorine atom at the 2-position and a chlorine atom at the 4-position of the benzene ring of *N*-isoxazolinylphenyl-triazinones was found to be conducive to bioactivity.²³ Therefore, in the present study, we mainly make the structural modification on the isoxazoline ring of *N*-phenylisoxazoline-thiadiazolo[3,4-*a*]pyridazines. To explore the effect of substituents on herbicidal activity, we performed four rounds of optimizations of the hybrids. First, compounds 1a–c with different functional groups at R^1 (H or $-CH_3$) and R^2 were synthesized as we previously showed that substituting the

Scheme 2. Synthesis of Compounds 2–3^a

^aReagents and conditions: (a) H₂SO₄, HOAc, H₂O, 100 °C; (b) R⁴I or R⁴Br, K₂CO₃, DMF, rt; (c) R⁵NH₂, hexafluorophosphate (HATU), *N,N*-diisopropylethylamine (DIPEA), CH₂Cl₂, rt; (d) Fe, NH₄Cl, C₂H₅OH (90%), reflux; (e) CCl₄, Et₃N, toluene, 0 °C-reflux; (f) hexahydropyridazine dihydrochloride, NaOH, toluene, H₂O, 0 °C; and (g) CO(OCCl₃)₂, Et₃N, acetone, 0 °C.

Scheme 3. Synthesis of Compound 5^a

^aReagents and conditions: (a) Et₃N, rt 0 °C; (b) toluene, Et₃N, rt.

methyl group at R¹ would be favorable to herbicidal activity. Then, we synthesized compounds 2 and 3, which had ester groups and amide groups at R², respectively. Moreover, we explored the new chemical space of the isoxazoline ring using a ring-closure strategy and generated compounds 4a–b. Finally, based on the degradation mechanism of fluthiacet-methyl in weeds,¹³ we thus proposed that compounds 1–4 might also be the proherbicides. To test this hypothesis, we synthesized a triazolo[3,4-*a*]pyridazine-containing compound 5.

Chemistry. The organic synthesis of *N*-phenylisoxazoline-thiadiazolo[3,4-*a*]pyridazines is illustrated in Schemes 1 and 2. According to our previously described procedures,²³ compounds 1 and 4 can be obtained by commencing with 2-chloro-4-fluoro-5-nitrobenzaldehyde 6. After stirring 6 and hydroxylamine hydrochloride in ethanol–H₂O solution for about 2 h, intermediate 7 was obtained in a yield of 91%. Then, after chlorination and 1,3-dipolar cycloaddition reactions, the corresponding isoxazoline derivatives 8 were generated in yields of 22–98%. Subsequently, the nitro groups of 8 were reduced by Fe/NH₄Cl in the ethanol (90%) solution under reflux conditions to provide intermediates 9. Finally, 9 reacted with CCl₄ in toluene to give the corresponding isothiocyanates, which were directly used in the next reaction step after removing the solvent. The isothiocyanates were then reacted with the hexahydropyridazine to afford the thiocarbamides. Cyclization of thiocarbamides in the presence of triphosgene in acetone with Et₃N as the catalyst provided 1 and 4 in good yields.

Initially, we tried to synthesize compounds 2 and 3 by adopting the esterification and amidation reactions, respectively. However, we found that compounds 2 were very unstable under the acid (H₂SO₄–H₂O) and base (NaOH, LiOH, and K₂CO₃) conditions (Table S2), and it was very hard to obtain the target carboxylic acid. Therefore, we designed another alternative synthetic route to synthesize 2 and 3. The methoxycarbonyl group of intermediate 8f was

hydrolyzed in a mixture of H₂SO₄, HOAc, and H₂O solution at 100 °C to obtain the corresponding carboxylic acid 10. Then, 10 reacted with R⁴I or R⁴Br in *N,N*-dimethylformamide (DMF) with potassium carbonate as a base to provide intermediates 11. The nitro intermediates 13 were obtained by reacting 10 with R⁵NH₂ in the presence of *O*-(7-azabenzotriazol-1-yl)-*N,N,N',N'*-tetramethyluronium hexafluorophosphate (HATU), *N,N*-diisopropylethylamine (DIPEA), and CH₂Cl₂ at room temperature. The amide compounds 12 and 14 were obtained using similar methods as 9. The target compounds 2 and 3 were prepared using similar synthetic routes as 1 and 4.

The synthetic route for the proposed active metabolite 5 is shown in Scheme 3. Reacting hexahydropyridazine dihydrochloride with ethyl carbonochloridate in CH₂Cl₂ with Et₃N as a base provided *N*-ethoxycarbonylhexahydropyridazine 15. Without further purification, 15 reacted with isothiocyanate 16 in toluene, and an intramolecular ring closure in the presence of Et₃N gave compound 5.

Herbicidal Activity and SARs. As we have envisaged that designing inhibitors by mimicking 3/4 of the structure of protoporphyrinogen IX would show higher herbicidal activity, after the structural superimposition of the *N*-phenylisoxazoline-thiadiazolo[3,4-*a*]pyridazine scaffold and the substrate of PPO, we found that thiadiazolo[3,4-*a*]pyridazine, a benzene ring, and an isoxazoline ring can each overlay with a pyrrole ring of the protoporphyrinogen IX, suggesting that the designed hybrids may have good herbicidal activity. Inspired by this, a series of substituents were introduced at R¹–R³ of the isoxazoline ring according to their chemical diversity and synthetic accessibility. The results indicated that most of the synthesized hybrids exhibited excellent broadleaf weed control; even at an extremely low usage rate of 9.375 g ai/ha, some compounds displayed a wider spectrum of weed control than that of fluthiacet-methyl at the rate of 9.375 g ai/ha.

Table 2. Post-Emergent Herbicidal Activity and NtPPO-Inhibitory Activity of Compounds 2


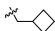
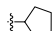
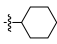
compd	R ⁴	dosage g ai/ha	% inhibition				K _i /nM	CLogP
			ABUJU ^a	AMARE	ECHCG	DIGSA		
2a	-CH ₃	37.5	100	100	69	27	33±64	
		18.75	100	100	48	25		
		9.375	100	95	40	20		
2b	-CH ₂ CH ₃	37.5	100	100	93	8	21.8±2.7	4.9
		18.75	100	96	77	0		
		9.375	100	81	72	0		
2c	-CH ₂ CH ₂ CH ₃	37.5	100	100	53	14	15±1.4	5.5
		18.75	100	100	31	0		
		9.375	100	95	13	0		
2d	-CH ₂ CH ₂ CH ₂ CH ₃	37.5	100	100	46	31	13.7±2.5	6.0
		18.75	100	100	41	25		
		9.375	100	100	37	21		
2e	-CH(CH ₃) ₂	37.5	100	100	43	34	7.6±0.2	5.2
		18.75	100	97	23	14		
		9.375	100	73	0	5		
2f	-CH ₂ CH ₂ F	37.5	100	94	41	0	22±5.5	4.6
		18.75	100	91	36	0		
		9.375	98	90	30	0		
2g	-CH ₂ CH ₂ CH ₂ F	37.5	100	100	48	23	87±9.4	4.9
		18.75	100	99	44	14		
		9.375	100	90	8	0		
2h	-CH ₂ CH=CH ₂	37.5	100	100	67	30	21±2.6	5.2
		18.75	100	95.8	37	15		
		9.375	100	85.3	24	13		
2i	-CH ₂ CH=C(CH ₃) ₂	37.5	100	100	73	44	30±11	6.1
		18.75	100	100	60	35		
		9.375	94	86	57	19		
2j	-CH ₂ C≡CH	37.5	100	100	72	43	33±6.2	4.5
		18.75	100	100	70	24		
		9.375	100	87	67	4		
2k	-CH ₂ CO ₂ C ₂ H ₅	37.5	100	100	41	31	15±2.8	4.8
		18.75	100	99	36	27		
		9.375	99	73	11	10		
2l	-CH(CH ₃)CO ₂ C ₂ H ₅	37.5	100	97	45	38	30±5.4	5.1
		18.75	100	86	26	22		
		9.375	100	83	21	18		
2m	-CF ₂ CO ₂ C ₂ H ₅	37.5	100	100	45	33	44±9.0	6.3
		18.75	100	93	31	26		
		9.375	100	92	27	18		
2n		37.5	100	100	59	18	28±6.3	5.4
		18.75	100	97	47	10		
		9.375	100	52	24	6		
2o		37.5	100	100	61	46	27±1.7	5.9
		18.75	100	84	39	25		
		9.375	100	72	20	10		
2p		37.5	100	100	69	38	16±2.8	5.9
		18.75	100	58	34	29		
		9.375	100	43	10	26		

Table 2. continued

compd	R ⁴	dosage g ai/ha	% inhibition				K _i /nM	CLogP
			ABUJU ^a	AMARE	ECHCG	DIGSA		
2q		37.5	100	99	53	24	17±3.1	5.9
		18.75	100	94	48	16		
		9.375	100	66	28	11		
2r	-CH ₂ C ₆ H ₅	37.5	100	100	39	49	27±2.2	6.1
		18.75	100	100	20	21		
		9.375	96	93	0	5		
2s	-CH ₂ C ₆ H ₅ (4-CH ₃)	37.5	100	99	28	18	24±5.0	6.6
		18.75	55	78	8	5		
		9.375	33	38	0	0		
2t	-CH ₂ C ₆ H ₅ (4-F)	37.5	100	100	41	61	48±9.4	6.2
		18.75	96	84	24	7		
		9.375	46	73	10	0		
2u	-CH ₂ C ₆ H ₅ (4-Cl)	37.5	100	100	53	37	23±2.0	6.8
		18.75	100	100	46	10		
		9.375	96	100	21	0		
2v	-CH ₂ C ₆ H ₅ (4-Br)	37.5	100	100	64	17	23±3.0	6.9
		18.75	92	99	29	11		
		9.375	39	74	0	0		
2w	-CH ₂ C ₆ H ₅ (4-CF ₃)	37.5	100	99	12	45	58±12	6.9
		18.75	24	32	0	38		
		9.375	12	22	0	12		
fluthiacet-methyl		37.5	100	100	52	46	15±0.2	3.8
		18.75	100	99	33	37		
		9.375	100	89	20	0		

^aAbbreviations: ABUJU: *A. juncea*; AMARE: *A. retroflexus*; DIGSA: *D. sanguinalis*; and ECHCG: *E. crus-galli*.

Table 3. Post-Emergent Herbicidal Activity and NtPPO-Inhibitory Activity of Compounds 3

compd	R ⁵	dosage g ai/ha	% inhibition				K _i /nM	cLogP
			ABUJU ^a	AMARE	ECHCG	DIGSA		
3a	-CH ₃	37.5	100	100	43.0	13.0	60 ± 10	3.8
		18.75	100	100	35.8	0		
		9.375	100	100	18.1	0		
3b	-CH ₂ CH ₃	37.5	100	100	34.9	25.0	24 ± 1.5	4.4
		18.75	100	90.5	30.0	15.0		
		9.375	100	87.2	0	9.3		
3c	-CH ₂ CH ₂ CH ₃	37.5	100	95.4	59.8	54.6	88 ± 12	4.9
		18.75	100	93.7	30.1	44.6		
		9.375	100	88.5	13.7	35.6		
3d	-CH ₂ CH ₂ CH ₂ CH ₃	37.5	100	40.6	0	27.5	48 ± 9.8	5.4
		18.75	100	39.1	0	25.8		
		9.375	100	30.0	0	11.1		
3e	-CH(CH ₃) ₂	37.5	100	61.8	49.3	15.1	70 ± 15	4.7
		18.75	100	54.7	41.9	12.3		
		9.375	100	47.6	30.0	3.2		
3f	-SO ₂ N(CH ₃)CH(CH ₃) ₂	37.5	100	57.5	65.3	40.7	22 ± 1.3	5.2
		18.75	100	43.4	51.1	31.7		
		9.375	89.4	34.8	27.4	25.0		
fluthiacet-methyl		37.5	100	100	51.5	45.8	15 ± 0.2	3.8
		18.75	100	98.7	33.4	37.2		
		9.375	100	88.5	19.9	0		

^aAbbreviations: ABUJU: *A. juncea*; AMARE: *A. retroflexus*; DIGSA: *D. sanguinalis*; and ECHCG: *E. crus-galli*.

First, we introduced an ethoxycarbonyl substitution at the R² position (**1a**) to partly match the 2-carboxyethyl group of the substrate. It was found that at the rate of 150 g ai/ha, **1a**

exhibited 100% control against ABUJU and AMARE by post-emergence application (Table 1), indicating that introducing substituents at R¹ and R² may be beneficial for herbicidal

Table 4. Post-Emergent Herbicidal Activity and NtPPO-Inhibitory Activity of Compounds 4a–b and 5

compd	R ¹	R ²	R ³	dosage g ai/ha	% inhibition				K _i /nM	cLogP
					ABUJU ^a	AMARE	ECHCG	DIGSA		
4a	H	–CH ₂ OCH ₂ –		150	100	100	79	74	10 ± 0.3	3.2
				37.5	100	99	76	70		
				18.75	100	95	58	66		
				9.375	100	92	49	45		
4b	H	–CH ₂ CH ₂ O–		150	100	100	86	87	18 ± 1.7	3.6
				37.5	100	100	80	60		
				18.75	100	100	56	55		
				9.375	100	92	48	46		
5				150	100	100	94	28	4.6 ± 1.1	4.5
				37.5	100	100	91	16		
				18.75	100	100	74	8		
				9.375	100	88	62	0		
fluthiacet-methyl				37.5	100	100	52	46	15 ± 0.2	3.8
				18.75	100	99	33	37		
				9.375	100	89	20	0		

^aAbbreviations: ABUJU: *A. juncea*; AMARE: *A. retroflexus*; DIGSA: *D. sanguinalis*; and ECHCG: *E. crus-galli*.

activity. Considering that there is a methyl group at the pyrrole ring of the substrate, we then introduced a methyl group at R¹ and synthesized compounds **1b** and **1c**. The results indicate that both **1b** and **1c** showed excellent herbicidal activity against the tested broadleaf weeds at 150 g ai/ha. Even at a rate as low as 9.375 g ai/ha, **1a–c** still exhibited 100% control against ABUJU and AMARE, implying that modifying the isoxazoline ring of the designed scaffold may be an effective approach to obtain highly potent compounds.

Second, as one of the design strategies of our compounds was to mimic parts of the substrate, so, in this round of optimization, we fixed R¹ as a methyl group and systematically optimized the substituents of R². In most cases, the ester-containing derivatives (**2a–e**) showed higher herbicidal activity than their corresponding amide-containing derivatives (**3a–e**) against the four kinds of tested weeds (Tables 2 and 3). A possible explanation for the decreased activity of the amide-substituted analogues is that the cLogP values of **3a–e** were lower than those of **2a–e** (Tables 2 and 3), which made it hard for weeds to absorb **3a–e** than **2a–e**. We noted that the ester-substituted compounds (**2a–d**) exhibited excellent herbicidal activity against the tested ABUJU and AMARE at 9.375–37.5 g ai/ha; especially, **2b** showed higher levels of ECHCG control than fluthiacet-methyl. Next, by either varying the length of ester side chains or modifying the size of ester groups, we designed and synthesized another 18 derivatives (**2f–w**). Half of the 18 compounds exhibited over 80% control of the tested broadleaf weeds at 9.375–37.5 g ai/ha (Table 2). Herbicidal potency decreased with increasing length of the ester side chains; hence, **2j** showed higher activity than **2k**. It was also found that the increased size of the ester group at R² exerted an adverse impact on herbicidal activity. For example, **2n** and **2o** displayed higher weed control than **2p**. Additionally, for compounds with (substituted)benzyl groups (**2r–w**) at R², substituting methyl (**2s**) or trifluoromethyl (**2w**) groups at the *para*-position was found to show substantial decreases in potency. Halogenated derivatives **2t** and **2v** showed lower broadleaf weed control than **2r**, whereas **2u** regained most of the herbicidal potency relative to **2r**.

Third, considering that our above optimization mainly focused on optimizing the side chains of R¹ and R², we therefore synthesized compounds **4a–b** by ring closure of R²

and R³. As shown in Table 4, both **4a** and **4b** displayed over 90% control against the tested ABUJU and AMARE at 9.375–150 g ai/ha. Additionally, **4a–b** also exhibited stronger ECHCG and DIGSA control compared with fluthiacet-methyl. Taken together, our results suggested that *N*-phenylisoxazoline-thiadiazolo[3,4-*a*]pyridazine was a privileged scaffold for novel herbicide discovery.

Finally, we changed the thiadiazolo[3,4-*a*]pyridazine moiety of the designed scaffold to triazolo[3,4-*a*]pyridazine and synthesized a representative compound **5**. As illustrated in Tables 4 and 5 displayed over 90% control against the ABUJU, AMARE, and ECHCG at the rates of 37.5–150 g ai/ha, which were comparable to that of its counterpart **2b**. Even at a rate as low as 9.375 g ai/ha, **5** still exhibited the same equipotency as **2b** for controlling ABUJU, slightly improved activity than **2b** in suppressing AMARE, and slightly decreased potency in inhibiting ECHCG relative to **2b**. These results indicated

Table 5. Crop Selectivity of Representative *N*-Phenylisoxazoline-thiadiazolo[3,4-*a*]pyridazines^a

compd	maize	soybean	sorghum	wheat	peanut	rice
2a	5	20	30	20	80	30
2b	10	50	70	30	60	30
2c	10	50	50	20	50	30
2d	15	60	70	30	40	30
2f	5	40	20	20	50	30
2g	10	20	20	20	60	30
2h	15	40	40	20	50	30
2i	15	40	30	20	50	30
2j	5	30	30	20	60	30
2l	10	20	20	20	30	30
2m	10	40	50	30	50	30
2r	10	20	30	15	50	15
2u	10	15	20	15	50	30
3a	5	50	20	15	40	30
3b	10	50	20	15	50	30
3c	20	80	70	20	70	30
fluthiacet-methyl	5	20	90	15	50	40

^aPost-emergent, 75 g ai/ha, data are presented as injury percentage/%.

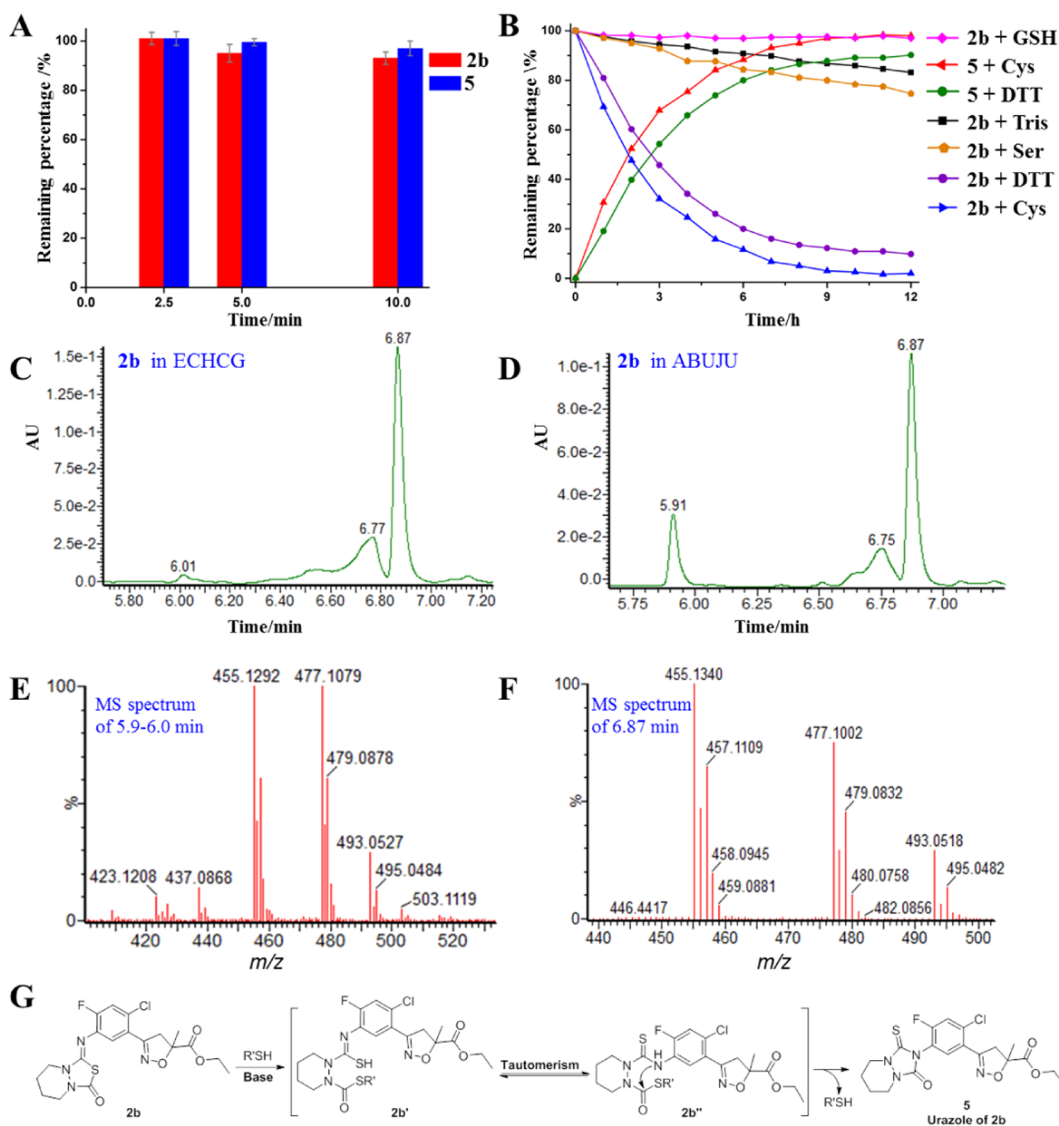


Figure 4. Stability and metabolism studies of **2b** in solutions and in vivo. (A) Chemical stability test of **2b** and **5** in NtPPO activity assay solution. (B) Decomposition of **2b** in Tris solution (20 mM, pH 8) in the presence of various reducing agents, GSH, Cys, DTT, and Ser. (C) Ultra performance liquid chromatography (UPLC) analysis of the ECHCG leaf extract after treating with **2b**. (D) UPLC analysis of the ABUJU leaf extract after treating with **2b**. (E) MS spectrum analysis of (C) and (D) at around 5.9–6.0 min. (F) MS spectrum analysis of (C) and (D) in 6.87 min. (G) Proposed isomerization of **2b** to **5** by reducing agents.

that **5** might be the herbicidally active metabolite of **2b** in vivo.^{12,13}

Herbicidal Spectrum. As we have discussed in the above section, many compounds displayed excellent broadleaf weed control at 9.375 g ai/ha. Among them, **2b** also exhibited over 90% control against the tested ECHCG at 37.5 g ai/ha. Considering the structural diversity, synthetic accessibility, and herbicidal activity, **2b** and **3a** were selected as representatives for further herbicidal spectrum studies. As shown in Figure 3a, **2b** and **3a** exhibited complete control against 16 and 15 kinds of 33 tested weeds at 75 g ai/ha, respectively. Even at an application rate as low as 12 g ai/ha, both **2b** and **3a** still displayed over 80% control of the 13 kinds of tested weeds. The averaged percent of weed control at 75, 30, and 12 g ai/ha for **2b** was 86.8, 76.2, and 57.3%, respectively, that for **3a** was 76.5, 61.7, and 51.2%, respectively, and that for fluthiacet-methyl was 72.3, 62.7, and 52.4%, respectively. Our results

indicated that **2b** had a slightly higher level of herbicidal potency than that of fluthiacet-methyl at 12–75 g ai/ha.

Crop Selectivity. Sixteen representative compounds (**2a–d**, **2f–i**, **2j**, **2l–m**, **2r–u**, and **3a–c**) with excellent broadleaf weed control (ABUJU and AMARE) were selected for further crop safety evaluation (Table 5). Among the tested crops, maize exhibited relatively high tolerance to **2a–c**, **2f–g**, **2j**, **2l–m**, **2r–u**, **3a–b**, and fluthiacet-methyl at 75 g ai/ha by post-emergence application, whereas soybean, sorghum, wheat, peanut, and rice were more sensitive to these compounds under the same test conditions. Collectively, our results indicated that **2a–c**, **2f–g**, **2j**, **2l–m**, **2r–u**, and **3a–b** might be used as novel herbicides for broadleaf weed control in maize fields.

PPO-Inhibitory Activity. Next, we tested the NtPPO-inhibitory activity of the synthesized compounds **1–5** to further evaluate whether these compounds are potent PPO inhibitors in vitro or not. The results indicated that most of the

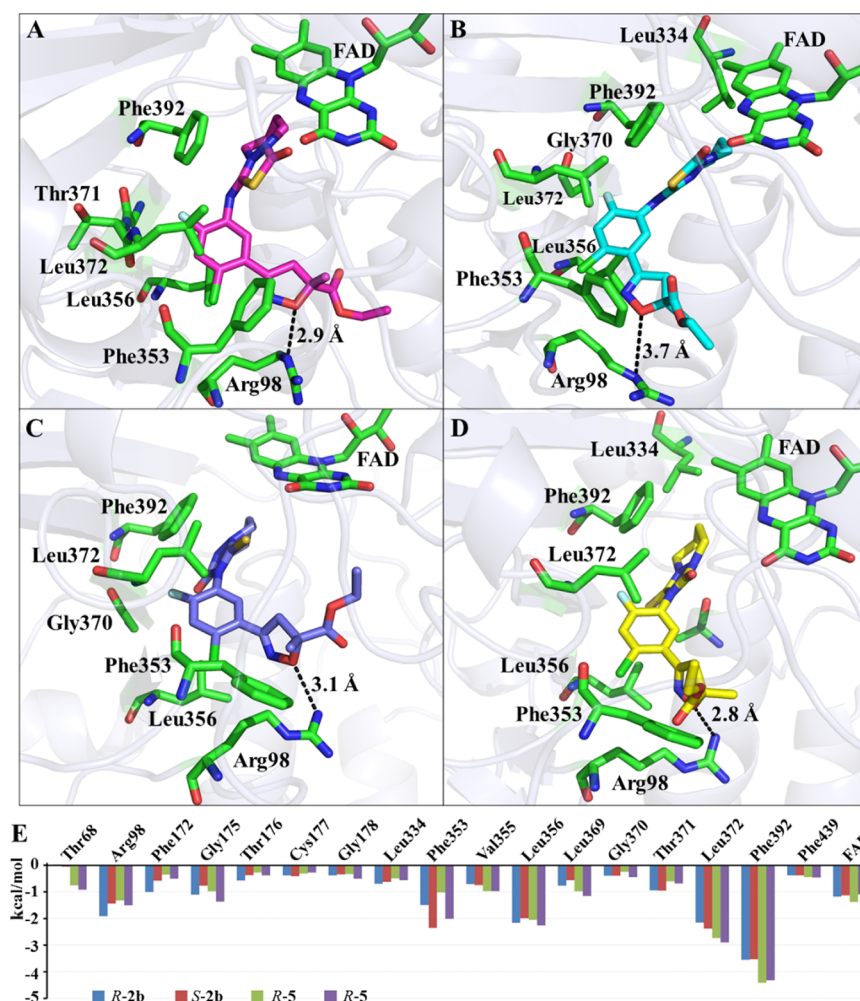


Figure 5. Molecular simulation studies of (R and S) **2b** and (R and S) **5** with NtPPO (pdb id: 1sez). (A) Binding mode of the R-**2b**-NtPPO complex; R-**2b** is shown as magenta sticks. (B) Binding mode of the S-**2b**-NtPPO complex; S-**2b** is shown as cyan sticks. (C) Binding mode of the R-**5**-NtPPO complex; R-**5** is shown as cyan sticks. (D) Binding mode of the S-**5**-NtPPO complex; S-**5** is shown as slate sticks. (E) Comparison of the total interaction binding energies (kcal/mol) of (R and S) **2b** and (R and S) **5** complexed with NtPPO.

synthesized *N*-phenylisoxazoline-thiadiazolo[3,4-*a*] pyridazines exhibited strong inhibition toward NtPPO activity (Tables 1–4). For example, **1b** ($K_i = 4.8$ nM) displayed 3-fold more potency than fluthiacet-methyl ($K_i = 15$ nM); **2d** ($K_i = 4.8$ nM) showed nearly 2-fold higher potency than fluthiacet-methyl. In general, compounds with excellent weed control in the greenhouse experiments also exhibited strong inhibitory potential against NtPPO, suggesting that the synthesized compounds **1–5** decimated weeds through inhibiting PPO *in planta*.

It was found that installing a methyl group at R¹ was beneficial to PPO-inhibitory activity (**1b** and **2b**), and increasing the length of the aliphatic chain at R⁴ was also favorable to activity (**2a–d**). While incorporation of a fluorine atom at the terminal $-\text{CH}_3$ of ethyl (**2b**) or *n*-propyl (**2c**) groups impaired the inhibitory activity, substituting the $-\text{CH}_3$ of ethyl group of **2b** with hydrophobic groups, such as $-\text{CH}=\text{CH}_2$ (**2h**) and $-\text{CH}=\text{C}(\text{CH}_3)_2$ (**2i**), was also found to be detrimental to activity. Additionally, changing the ester groups (**2a–e**) of R² to their relative amide groups (**3a–e**) eroded inhibition activity, indicating that both the absorption property and the PPO-inhibitory potency of the synthesized hybrids are important to achieve excellent herbicidal activity.

Stability and Activation Mechanism Studies of **2b**.

In the enzymatic study, we have found that compound **5** ($K_i = 4.6$ nM) showed 4-fold more activity than **2b** ($K_i = 21.8$ nM) in inhibiting NtPPO activity. Additionally, both **2b** and **5** showed excellent broadleaf weed control at a rate as low as 9.375 g ai/ha. To check whether **2b** can be transformed into **5**, we performed stability and metabolism studies of **2b**. First, we tested the stability of **2b** in PBS (pH 7.4, 10 mM) and an NtPPO activity assay solution. The results indicated that **2b** showed high stability in PBS solution; almost no hydrolysis was observed after 12 h (Figure S1). In contrast to **2b**, only about 5% of **5** was decomposed in the PBS solution after 12 h, indicating that **2b** showed a relatively lower hydrolysis rate than **5** in PBS solution. Interestingly, **5** showed higher stability than **2b** in NtPPO assay solution (Figure 4A). On incubating **2b** and **5** in the NtPPO assay solution for 2.5 min, no hydrolysis of the two compounds was observed; in 5 min, about 5 and 0.5% of **2b** and **5** were decomposed, respectively. As in the NtPPO enzymatic process, a linear increase in fluorescence of protoporphyrin IX occurred generally in 3 min; therefore, the hydrolysis of **2b** in the assay solution almost did not affect its PPO-inhibitory activity.

Second, we tested whether **2b** converted into **5** in the Tris solution (20 mM, pH 8.0) in the presence of various reducing agents (Figure 4B).¹³ It was found that the stability of **2b** was decreased with the increase of pH values, as 17% of **2b** was decomposed in the Tris solution in 12 h. However, GSH could inhibit the hydrolysis of **2b**, whereas Ser could accelerate the hydrolysis of **2b**. Furthermore, no **5** was detected in Tris, GSH-, and Ser-Tris solutions, suggesting that the conversion of **2b** into **5** could not occur under these conditions. We observed that both Cys and DTT could promote the isomerization of **2b** to **5** in the Tris solution, while Cys showed a faster conversation rate than DTT. As illustrated in Figure 4B, in 1 h, about 20% of **2b** in the DTT-Tris solution was isomerized to **5**, and about 30% of **2b** in the Cys-Tris solution was converted into **5**. The conversion of **2b** into **5** in Cys-Tris solution peaked in 9 h and completed in 12 h. However, 10% of **2b** still remained in the DTT-Tris solution in 12 h. One possible explanation for the decreased isomerization rate of DTT relative to Cys was that the bulky *N*-phenylisoxazoline moiety of **2b** would block the nucleophilic substitution reaction of DTT.

Third, to understand whether **5** is the active metabolite of **2b** *in planta* or not, we used ultra-high performance liquid chromatography coupled high resolution mass spectrometry (UPLC-HRMS) to analyze the leaf extracts of two representative weeds (ECHCG and ABUJU) after treating by **2b**. About 2 h post-treatment, the leaves of ABUJU began to drop; therefore, the leaves of ABUJU and ECHCG were cut for further analysis. We observed that there were two new peaks with the retention times of 6.01 and 5.91 min in ECHCG (Figure 4C) and ABUJU (Figure 4D) extracts, respectively. Further study indicated that the two new peaks corresponded to compound **5** because the retention time and the HRMS spectrum (Figure 4E) of the two peaks were the same as those of **5** (Figure S2). Compound with a retention time of 6.87 min in Figure 4C,D was identified as **2b** by analyzing its HMRS spectrum (Figure 4F). Additionally, we found that about 27% of **2b** was converted into **5** in ABUJU, whereas only 10% of **2b** was isomerized to **5** in ECHCG. These results indicated that **5** was the bioactive metabolite of **2b**, and as weeds contained more **5** *in vivo*, faster toxic effects were observed.

Base on the above discussions, we proposed a conversion mechanism of **2b** into **5** by reducing agents. The isomerization began with the nucleophilic attack of the carbonyl group of the thiadiazolo[3,4-*a*]pyridazine ring by reducing agents. The resulting reaction intermediate **2b'** could isomerize to **2b''** in the solution and then after an intramolecular nucleophilic substitution reaction, **5** was formed (Figure 4G).³⁹

Molecular Simulation Analysis. For further elucidating the molecular basis of **2b** and **5**, we performed molecular simulation studies of **2b**- and **5**-NtPPO systems. As there are chiral centers in the isoxazoline ring of **2b** and **5**, the binding modes and free energies of both the *R* and *S* isomers of the two compounds were studied. After docking (*R* and *S*) **2b** and (*R* and *S*) **5** into the active site of NtPPO using AutoDock 4.2, reasonable binding modes of these compounds were selected for further MD simulations (Figure S3). The average binding energies of *R*-**2b**, *S*-**2b**, *R*-**5**, and *S*-**5** with NtPPO were −30.97, −28.91, −31.95, and −30.73 kcal/mol, respectively (Table S1), suggesting that the *R* configurations of **2b** and **5** were slightly more active than the *S* configurations. Additionally, our calculation results also indicated that **5** showed higher binding

affinity than **2b**, which was consistent with the trend of our NtPPO-inhibitory results.

Next, we compared the binding modes of *R*-**2b**, *S*-**2b**, *R*-**5**, and *S*-**5** with NtPPO. Representative snapshots of the four compounds were taken from the last frame of each simulation at 30 ns. As illustrated in Figure 5A–D, there were no major differences in the binding modes of the four compounds. For example, the thiadiazolo[3,4-*a*]pyridazine ring of *R*-**2b** (Figure 5A) and *S*-**2b** (Figure 5B) could form stable π – π interactions with Phe392; the same interactions were also observed in *R*-**5** (Figure 5C) and *S*-**5** (Figure 5D). The benzene rings of the four compounds formed hydrophobic interactions with Leu356 and Leu372, which in turn decreased the influence of ΔG_{sol} and enhanced the contribution of ΔE_{VDW} . Furthermore, the oxygen atoms on the isoxazoline rings of the four compounds formed hydrogen-bonding interactions with Arg98. Besides, the isoxazoline rings of the four compounds formed T– π interactions with Phe353. These T– π interactions could stabilize the binding modes and be advantageous to the PPO-inhibitory activity.

To gain additional insights into the differences in the interactions of *R*-**2b**, *S*-**2b**, *R*-**5**, and *S*-**5** with the key amino acids of NtPPO, we performed decomposition free-energy calculations of the four complexes. As shown in Figure 5E, Arg98, Gly175, Phe353, Leu356, Leu372, Phe392, and FAD made most of the contribution to the binding free energies of the four compounds. Among them, Phe392 contributed the largest proportion to the binding energies, suggesting that the design of new compounds that could form stronger π – π interactions with Phe392 would have higher PPO-inhibitory activity. Additionally, the energy contributions of Thr68, Leu372, and Phe392 in *R*-**5**– and *S*-**5**–NtPPO complexes were improved compared with that of *R*-**2b**– and *S*-**2b**–NtPPO complexes. We inferred that these improvements could improve the NtPPO-inhibitory activity of **5** directly.

In conclusion, a new *N*-phenylisoxazoline-thiadiazolo[3,4-*a*]pyridazine herbicidal active scaffold was generated by hybridizing the scaffold of *N*-isoxazolinylphenyltriazinone and fluthiacet-methyl. Most of the synthesized compounds showed excellent weed control at 9.375–150 g ai/ha by the post-emergent application. Several of them showed improved NtPPO-inhibitory activity compared with fluthiacet-methyl. Promisingly, compound **2b** showed higher weed control than fluthiacet-methyl at the rate of 12–75 g ai/ha. Additionally, **2b** was also selective to maize at 75 g ai/ha by the post-emergence application. Our mechanism studies indicated that *in planta* **2b** could rapidly isomerize to compound **5** (urazole of **2b**), which might be the bioactive metabolite of **2b**. Because **5** ($K_i = 4.6$ nM) exhibited 4.6-fold higher potency than **2b** ($K_i = 21.8$ nM) in inhibiting the activity of NtPPO, due to the faster isomerization rate of **2b** to **5** in weeds, more obvious injury symptoms were observed. The results of MD simulations indicated that **5** showed stronger π – π interaction with Phe392 than **2b**. Our study not only provides a promising lead compound for weed control in maize fields but is also useful to understand the molecular mechanisms and the basis of thiadiazole-type PPO herbicides.

■ ASSOCIATED CONTENT

Supporting Information

The Supporting Information is available free of charge at <https://pubs.acs.org/doi/10.1021/acs.jafc.0c05955>.

Detailed synthetic procedures, ^1H and ^{13}C NMR, and high-resolution mass spectra (HRMS) of compounds **1–4**; calculated binding free energies (kcal/mol) of **R-2b**, **S-2b**, **R-5**, and **S-5** with NtPPO (Table S1); optimization of the ester hydrolysis reaction conditions of **2a** (Table S2); chemical stability of compounds **2b** and **5** in PBS (pH 7.4, 10 mM) solution (Figure S1); UPLC-MS analysis of compound **5** (Figure S2); and root-mean-square deviation (RMSD) analysis of **R-2b**, **S-2b**, **R-5**, **S-5**, and NtPPO systems (Figure S3) (PDF)

AUTHOR INFORMATION

Corresponding Authors

Da-Wei Wang — State Key Laboratory of Elemento-Organic Chemistry and Department of Chemical Biology, National Pesticide Engineering Research Center, Collaborative Innovation Center of Chemical Science and Engineering, College of Chemistry, Nankai University, Tianjin 300071, P. R. China; Phone: +86 022-23504782; Email: wangdw@nankai.edu.cn

Zhen Xi — State Key Laboratory of Elemento-Organic Chemistry and Department of Chemical Biology, National Pesticide Engineering Research Center, Collaborative Innovation Center of Chemical Science and Engineering, College of Chemistry, Nankai University, Tianjin 300071, P. R. China; orcid.org/0000-0002-3332-5413; Phone: +86 022-23504782; Email: zhenxi@nankai.edu.cn

Authors

Rui-Bo Zhang — State Key Laboratory of Elemento-Organic Chemistry and Department of Chemical Biology, National Pesticide Engineering Research Center, Collaborative Innovation Center of Chemical Science and Engineering, College of Chemistry, Nankai University, Tianjin 300071, P. R. China

Shu-Yi Yu — State Key Laboratory of Elemento-Organic Chemistry and Department of Chemical Biology, National Pesticide Engineering Research Center, Collaborative Innovation Center of Chemical Science and Engineering, College of Chemistry, Nankai University, Tianjin 300071, P. R. China

Lu Liang — State Key Laboratory of Elemento-Organic Chemistry and Department of Chemical Biology, National Pesticide Engineering Research Center, Collaborative Innovation Center of Chemical Science and Engineering, College of Chemistry, Nankai University, Tianjin 300071, P. R. China

Ismail Ismail — State Key Laboratory of Elemento-Organic Chemistry and Department of Chemical Biology, National Pesticide Engineering Research Center, Collaborative Innovation Center of Chemical Science and Engineering, College of Chemistry, Nankai University, Tianjin 300071, P. R. China

Yong-Hong Li — State Key Laboratory of Elemento-Organic Chemistry and Department of Chemical Biology, National Pesticide Engineering Research Center, Collaborative Innovation Center of Chemical Science and Engineering, College of Chemistry, Nankai University, Tianjin 300071, P. R. China

Han Xu — State Key Laboratory of Elemento-Organic Chemistry and Department of Chemical Biology, National Pesticide Engineering Research Center, Collaborative Innovation Center of Chemical Science and Engineering,

College of Chemistry, Nankai University, Tianjin 300071, P. R. China

Xin Wen — State Key Laboratory of Elemento-Organic Chemistry and Department of Chemical Biology, National Pesticide Engineering Research Center, Collaborative Innovation Center of Chemical Science and Engineering, College of Chemistry, Nankai University, Tianjin 300071, P. R. China

Complete contact information is available at:
<https://pubs.acs.org/10.1021/acs.jafc.0c05955>

Notes

The authors declare no competing financial interest.

ACKNOWLEDGMENTS

This research was funded in part by the National Key Research and Development Program of China (No. 2017YFD0200501) and the National Natural Science Foundation of China (Nos. 21702111, 22077072, 21672118, 21332004, and 21877066).

REFERENCES

- (1) Lamberth, C.; Jeanmart, S.; Luksch, T.; Plant, A. Current challenges and trends in the discovery of agrochemicals. *Science* **2013**, *341*, 742–746.
- (2) Yang, R.; Lv, M.; Xu, H. Synthesis of piperine analogs containing isoxazoline/pyrazoline scaffold and their pesticidal bioactivities. *J. Agric. Food Chem.* **2018**, *66*, 11254–11264.
- (3) Salas, R. A.; Burgos, N. R.; Tranel, P.; Singh, S.; Glasgow, L.; Scott, R. C.; Nichols, R. L. Resistance to PPO-inhibiting herbicide in *Palmer amaranth* from Arkansas, USA. *Pest Manage. Sci.* **2016**, *72*, 864–869.
- (4) Yoon, J.; Han, Y.; Ahn, Y. O.; Hong, M. K.; Sung, S. K. Characterization of HemY-type protoporphyrinogen IX oxidase genes from cyanobacteria and their functioning in transgenic Arabidopsis. *Plant Mol. Biol.* **2019**, *101*, 561–574.
- (5) Wang, B. F.; Wen, X.; Qin, X. H.; Wang, Z. F.; Tan, Y.; Shen, Y. Q.; Xi, Z. Quantitative structural insight into human variegate porphyria disease. *J. Biol. Chem.* **2013**, *288*, 11731–11740.
- (6) Park, J.; Ahn, Y. O.; Nam, J. W.; Hong, M. K.; Song, N.; Kim, T.; Yu, G. H.; Sung, S. K. Biochemical and physiological mode of action of tiafenacil, a new protoporphyrinogen IX oxidase-inhibiting herbicide. *Pestic. Biochem. Physiol.* **2018**, *152*, 38–44.
- (7) Patzoldt, W. L.; Hager, A. G.; McCormick, J. S.; Tranel, P. J. A codon deletion confers resistance to herbicides inhibiting protoporphyrinogen oxidase. *Proc. Natl. Acad. Sci. U.S.A.* **2006**, *103*, 12329–12334.
- (8) Brzezowski, P.; Ksas, B.; Havaux, M.; Grimm, B.; Chazaux, M.; Peltier, G.; Johnson, X.; Alric, J. The function of Protoporphyrinogen IX Oxidase in chlorophyll biosynthesis requires oxidised plastoquinone in *Chlamydomonas reinhardtii*. *Commun. Boil.* **2019**, *2*, 159.
- (9) Zuo, Y.; Wu, Q.; Su, S. W.; Niu, C. W.; Xi, Z.; Yang, G. F. Synthesis, herbicidal activity, and QSAR of novel *N*-benzothiazolylpyrimidine-2,4-diones as protoporphyrinogen oxidase inhibitors. *J. Agric. Food Chem.* **2016**, *64*, 552–562.
- (10) Zhao, L. X.; Jiang, M. J.; Hu, J. J.; Zou, Y. L.; Cheng, Y.; Ren, T.; Gao, S.; Fu, Y.; Ye, F. Design, synthesis, and herbicidal activity of novel diphenyl ether derivatives containing fast degrading tetrahydrophthalimide. *J. Agric. Food Chem.* **2020**, *68*, 3729–3741.
- (11) Reddy, S. S.; Stahlman, P. W.; Geier, P. W.; Bean, B. W.; Dozier, T. Grain sorghum response and *Palmer amaranth* control with postemergence application of fluthiacet-methyl. *Int. J. Pest Manage.* **2014**, *60*, 147–152.
- (12) Jeschke, P. Pesticides and their use as agrochemicals. *Pest Manage. Sci.* **2016**, *72*, 210–225.
- (13) Shimizu, T.; Hashimoto, N.; Nakayama, I.; Nakao, T.; Mizutani, H.; Unai, T.; Yamaguchi, M.; Abe, H. A novel isourazole

herbicide, fluthiacet-methyl, is a potent inhibitor of protoporphyrinogen oxidase after isomerization by glutathione S-transferase. *Plant Cell Physiol.* **1995**, *36*, 625–632.

(14) Hao, G. F.; Tan, Y.; Yang, S. G.; Wang, Z. F.; Zhan, C. G.; Xi, Z.; Yang, G. F. Computational and experimental insights into the mechanism of substrate recognition and feedback inhibition of protoporphyrinogen oxidase. *PLoS One* **2013**, *8*, No. e69198.

(15) Hao, G. F.; Zuo, Y.; Yang, S. G.; Yang, G. F. Protoporphyrinogen oxidase inhibitor: an ideal target for herbicide discovery. *Chimia* **2011**, *65*, 961–969.

(16) Wang, B. F.; Wen, X.; Xi, Z. Molecular simulations bring new insights into protoporphyrinogen IX oxidase/protoporphyrinogen IX interaction modes. *Mol. Inf.* **2016**, *35*, 476–482.

(17) Tan, Y.; Sun, L.; Xi, Z.; Yang, G. F.; Jiang, D. Q.; Yan, X. P.; Yang, X.; Li, H. Y. A capillary electrophoresis assay for recombinant *Bacillus subtilis* protoporphyrinogen oxidase. *Anal. Biochem.* **2008**, *383*, 200–204.

(18) Koch, M.; Breithaupt, C.; Kiefersauer, R.; Freigang, J.; Huber, R.; Messerschmidt, A. Crystal structure of protoporphyrinogen IX oxidase: a key enzyme in haem and chlorophyll biosynthesis. *EMBO J.* **2004**, *23*, 1720–1728.

(19) Hao, G. F.; Tan, Y.; Xu, W. F.; Cao, R. J.; Xi, Z.; Yang, G. F. Understanding resistance mechanism of protoporphyrinogen oxidase-inhibiting herbicides: insights from computational mutation scanning and site-directed mutagenesis. *J. Agric. Food Chem.* **2014**, *62*, 7209–7215.

(20) Wang, D. W.; Li, Q.; Wen, K.; Ismail, I.; Liu, D. D.; Niu, C. W.; Wen, X.; Yang, G. F.; Xi, Z. Synthesis and herbicidal activity of pyrido[2,3-*d*]pyrimidine-2,4-dione-benzoxazinone hybrids as protoporphyrinogen oxidase inhibitors. *J. Agric. Food Chem.* **2017**, *65*, 5278–5286.

(21) Wang, D. W.; Zhang, R. B.; Ismail, I.; Xue, Z. Y.; Liang, L.; Yu, S. Y.; Wen, X.; Xi, Z. Design, herbicidal activity, and QSAR Analysis of cycloalka[*d*]quinazoline-2,4-dione-benzoxazinones as protoporphyrinogen IX oxidase inhibitors. *J. Agric. Food Chem.* **2019**, *67*, 9254–9264.

(22) Theodoridis, G.; Liebl, R.; Zagar, C. Protoporphyrinogen IX Oxidase Inhibitors. In *Modern Crop Protection Compounds*; Wiley-VCH Verlag GmbH & Co. KGaA, 2012; pp 163–195.

(23) Wang, D. W.; Zhang, R. B.; Yu, S. Y.; Liang, L.; Ismail, I.; Li, Y. H.; Xu, H.; Wen, X.; Xi, Z. Discovery of novel *N*-isoxazolinyphenyl-triazinones as promising protoporphyrinogen IX oxidase inhibitors. *J. Agric. Food Chem.* **2019**, *67*, 12382–12392.

(24) Wang, D. W.; Lin, H. Y.; He, B.; Wu, F. X.; Chen, T.; Chen, Q.; Yang, W. C.; Yang, G. F. An efficient one-pot synthesis of 2-(aryloxyacetyl)cyclohexane-1,3-diones as herbicidal 4-hydroxyphenylpyruvate dioxygenase inhibitors. *J. Agric. Food Chem.* **2016**, *64*, 8986–8993.

(25) Wang, D. W.; Lin, H. Y.; Cao, R. J.; Ming, Z. Z.; Chen, T.; Hao, G. F.; Yang, W. C.; Yang, G. F. Design, synthesis and herbicidal activity of novel quinazoline-2,4-diones as 4-hydroxyphenylpyruvate dioxygenase inhibitors. *Pest Manage. Sci.* **2015**, *71*, 1122–1132.

(26) Wang, D. W.; Lin, H. Y.; Cao, R. J.; Chen, T.; Wu, F. X.; Hao, G. F.; Chen, Q.; Yang, W. C.; Yang, G. F. Synthesis and herbicidal activity of triketone-quinoline hybrids as novel 4-hydroxyphenylpyruvate dioxygenase inhibitors. *J. Agric. Food Chem.* **2015**, *63*, 5587–5596.

(27) Wang, D. W.; Lin, H. Y.; Cao, R. J.; Yang, S. G.; Chen, Q.; Hao, G. F.; Yang, W. C.; Yang, G. F. Synthesis and herbicidal evaluation of triketone-containing quinazoline-2,4-diones. *J. Agric. Food Chem.* **2014**, *62*, 11786–11796.

(28) Jiang, L. L.; Zuo, Y.; Wang, Z. F.; Tan, Y.; Wu, Q. Y.; Xi, Z.; Yang, G. F. Design and syntheses of novel *N*-(benzothiazol-5-yl)-4,5,6,7-tetrahydro-1*H*-isoindole-1,3(2*H*)-dione and *N*-(benzothiazol-5-yl)isoindoline-1,3-dione as potent protoporphyrinogen oxidase inhibitors. *J. Agric. Food Chem.* **2011**, *59*, 6172–6179.

(29) Hao, G. F.; Zuo, Y.; Yang, S. G.; Chen, Q.; Zhang, Y.; Yin, C. Y.; Niu, C. W.; Xi, Z.; Yang, G. F. Computational discovery of potent and bioselective protoporphyrinogen IX oxidase inhibitor via

fragment deconstruction analysis. *J. Agric. Food Chem.* **2017**, *65*, 5581–5588.

(30) Shepherd, M.; Dailey, H. A. A continuous fluorimetric assay for protoporphyrinogen oxidase by monitoring porphyrin accumulation. *Anal. Biochem.* **2005**, *344*, 115–121.

(31) Zhang, Y.; Wang, D.; Shen, Y.; Xi, Z. Crystal structure and biochemical characterization of *Striga hermonthica* hypo-sensitive to light 8 (ShHTL8) in strigolactone signaling pathway. *Biochem. Biophys. Res. Commun.* **2020**, *523*, 1040–1045.

(32) Henry, S.; Anand, J. P.; Twarozynski, J. J.; Brinkel, A. C.; Pogozheva, I. D.; Sears, B. F.; Jutkiewicz, E. M.; Traynor, J. R.; Mosberg, H. I. Aromatic-amine pendants produce highly potent and efficacious mixed efficacy mu-Opioid receptor (MOR)/delta-Opioid receptor (DOR) peptidomimetics with enhanced metabolic stability. *J. Med. Chem.* **2020**, *63*, 1671–1683.

(33) Jiang, B.; Jin, X.; Dong, Y.; Guo, B.; Cui, L.; Deng, X.; Zhang, L.; Yang, Q.; Li, Y.; Yang, X.; Smagghe, G. Design, synthesis, and biological activity of novel heptacyclic pyrazolamide derivatives: a new candidate of dual-target insect growth regulators. *J. Agric. Food Chem.* **2020**, *68*, 6347–6354.

(34) Tosco, P.; Balle, T.; Shiri, F. Open3DALIGN: an open-source software aimed at unsupervised ligand alignment. *J. Comput.-Aided Mol. Des.* **2011**, *25*, 777–783.

(35) DeLano, W. *The PyMOL Molecular Graphics System*; Delano Scientific: San Carlos, CA, 2002.

(36) Morris, G. M.; Huey, R.; Lindstrom, W.; Sanner, M. F.; Belew, R. K.; Goodsell, D. S.; Olson, A. J. AutoDock4 and AutoDockTools4: Automated docking with selective receptor flexibility. *J. Comput. Chem.* **2009**, *30*, 2785–2791.

(37) Case, D. A.; Babin, V.; Berryman, J. T.; Betz, R. M.; Cai, Q.; Cerutti, D. S.; Cheatham, T. E.; Darden, I. T. A.; Duke, R. E.; Gohlke, H.; Goetz, A. W.; Gusarov, S.; Homeyer, N.; Janowski, P.; Kaus, J.; Kolossváry, I.; Kovalenko, A.; Lee, T. S.; LeGrand, S.; Luchko, T.; Luo, R.; Madej, B.; Merz, K. M.; Paesani, F.; Roe, D. R.; Roitberg, A.; Sagui, C.; Salomon-Ferrer, R.; Seabra, G.; Simmerling, C. L.; Smith, W.; Swails, J.; Walker, R. C.; Wang, J.; Wolf, R. M. *AMBER 14*; University of California: San Francisco, 2014.

(38) Yang, J. F.; Yin, C. Y.; Wang, D.; Jia, C. Y.; Hao, G. F.; Yang, G. F. Molecular determinants elucidate the selectivity in abscisic acid receptor and HAB1 protein interactions. *Front. Chem.* **2020**, *8*, 425.

(39) Aizawa, H.; Brown, H. M. Metabolism and Degradation of Porphyrin Biosynthesis Inhibitor Herbicides. In *Peroxidizing Herbicides*; Böger, P.; Wakabayashi, K., Eds.; Springer-Verlag: Berlin-Heidelberg, 1999; pp 347–381.